Colloid Polym Sci 273:866–875 (1995)

ORIGINAL CONTRIBUTION

A. Müller
W. Burchard

Structure formation of surfactants in concentrated sulphuric acid: a light scattering study

Received: 11 April 1994
Accepted: 6 March 1995

Dr. A. Müller (✉)
Institute of Organic Chemistry
University of Greifswald
17489 Greifswald, FRG

W. Burchard
Institute of Macromolecular Chemistry
University of Freiburg
79104 Freiburg, FRG

Abstract A common cationic surfactant, *n*-hexadecylammonium hydrogensulphate, dissolved in concentrated sulphuric acid, has been studied by static and dynamic light scattering. Micelle formation has been observed even in this unusual solvent. An apparent molar mass of 45 500 ± 4.5% was found for the aggregates. A translational diffusion coefficient $D_0 = 5.5 \times 10^{-9}$ cm^2/s was measured which gave a hydrodynamically effective radius of $R_h = 17.7$ nm. The geometric radius of gyration was $R_g = 76.2$ nm. The ratio $R_g/R_h = 4.33$ is indicative for rodlike structures. Assuming a polydispersity of $L_w/L_n = 2$ this corresponds to a cylinder of $L_w = 152$ nm. An axial ratio $p_w = (L_w/d) = 60.4$ nm was estimated which leads to a cylinder diameter of 2.53 nm. At surfactant concentrations higher than 5% (w/vol) the rod-like micelles aggregate to form more globular structures. The time correlation function, recorded by dynamic light scattering, exhibited a two-step decay which indicates a bimodal distribution of particle sizes. The fast motion coincides with that of the micelles at low concentrations while the other is slower than the fast one by three orders of magnitude and corresponds to the translational motion of large clusters.

Key words *n*-hexadecylammonium hydrogensulphate – concentrated sulphuric acid as solvents – static light scattering – dynamic light scattering – micellar structures

Introduction

Cationic surfactants have been studied mostly in aqueous medium. Only a few studies are known which were made in concentrated sulphuric acid [1–5]. Recently, we published data on the critical micelle concentration (CMC) of various cationic surfactants, among others *n*-hexadecylammonium hydrogensulphate in concentrated sulphuric acid and in methane sulphonic acid [6–10]. The CMC in concentrated sulphuric acid was found to be considerably higher than in water. (The CMC in 96% H_2SO_4 is 1.57×10^{-3} mol/dm^{-3}). In methane sulphonic acid it was even more than one order of magnitude higher than in concentrated sulphuric acid [9]. It appeared of interest to us to get more information on the actual structure of these micellar aggregates.

Light scattering appears to be an appropriate method for studying such structures [11–16]. We applied the combination of static and dynamic light scattering, as described in a previous paper [17], to the surfactant dissolved in concentrated sulphuric acid. Experiments of this kind are not trivial for several reasons: First, one has to expect difficulties in preparing optically clear solutions because of the high viscosity of the concentrated sulphuric acid. Second, the water content of 4% in the sulphuric acid might cause a preferential adsorption. Finally, it was not clear from the beginning whether there would be enough

optical contrast to detect the excess scattering by the micelles.

We report here some striking observations which appeared to us worth publishing in spite of some uncertainties that arose from the mentioned difficulties. In preliminary measurements with *n*-hexadecyltrimethylammonium bromide we proved that light-scattering studies are possible with this unusual solvent. Unfortunately, the concentrated solutions developed an orange-red color which is typical of free bromine. We suspected that the observed structure formation in this solvent could be influenced by free bromine. For this reason, we changed the anion of the surfactant to hydrogensulphate. Light-scattering experiments with surfactants in concentrated sulphuric acid are rare, and to our knowledge there has been reported only one study prior to us by Steigman and Shane [4] who determined the CMC from the sudden increase of the scattering intensity when a certain concentration was surpassed.

Static light scattering allows the determination of the molar mass M_w, radius of gyration R_g and the second viral coefficient A_2, and dynamic light scattering gives the translation diffusion coefficient D [18] and information on the size distribution of the micelles from the so-called time correlation function (TCF) [11–18]. The combination of data measured by this method has been shown to give rather comprehensive information on the size and architecture of the particle in solution [19]. The techniques of static and dynamic light scattering have been frequently applied to characterizing micellar systems in aqueous media. Good overviews of huge literature were given by Candau [15] and Magid [16]. Some details on the techniques applied in this paper nevertheless will be outlined in a separate section to make for easier reading.

Materials and methods

A MOS quality of concentrated sulphuric acid (96%) from Baker B.V. (Deventer, Holland) was used. This solvent had already been filtered through 0.25 μm pore size, and could be used for light-scattering studies without further purification. In fact, the dust problem appeared far less significant than expected, possibly since organic material is efficiently degraded in this acid.

n-Hexadecylammonium hydrogensulphate was prepared by dissolving *n*-hexadecylamine in diethylether followed by precipitation with an excess of concentrated sulphuric acid. The precipitate was purified by repeated recrystallization from ethylacetate.

Light-scattering measurements were performed with concentrations in the range from 0.8 up to 20% (w/vol). The solutions were optically clarified by filtering through PTFE Milipore filters of 0.2 μm or 0.5 μm pore size (Milex-FGS and Milex-SR, respectively). Some solutions were used for measurements directly after filtering, but in most cases it turned out to be essential to wait for about 6 h before performing measurements. This was necessary because of the strong foam formation and to make sure that all air bubbles in the highly viscous medium had disappeared. Because of this principal difficulty the concentration of the surfactant was not determined again after filtration. There might be a small fraction detained in the filter which would lead to a lower molecular weight.

A fully automated and computer-controlled ALV 3000 photogoniometer equipped with a correlator/structurator by ALV Langen/Hessen, Germany, was used for the measurements. A Krypton ion laser type 2020 from Spectra Physics served as light source. The instrument is described in detail in a previous paper [17]. Cylindric cells of 8 mm diameter were used. The scattering intensity was measured in an angular regime from 30 to 150 degrees in steps of 10 degrees.

Measurements of the differential refractive index increment were made with a Brice-Phoenix differential refractometer at a wavelength of $\lambda_0 = 647$ nm identical with that of the laser used for LS measurements. A value of $dn/dc = 0.039$ was found and a refractive index $n_0 = 1.4247$ was measured for sulphuric acid. The kinematic viscosity at 20 °C was measured in a capillary viscometer and was recast in the true viscosity using the density that was measured directly with the density measuring instrument DMA 02/C by Anton Paar, Graz Austria. A value of 23.18 cp was obtained. This result is in good agreement with a viscosity of 22.79 cp that is obtained for 96% H_2SO_4 by extrapolation from tabulated data [20].

The dn/dc-value has to be considered as an apparent quantity. The small content of water might cause a strong preferential adsorption of water to the surfactant which would distort the correct equilibrium value needed for the molar mass determination of the micelles. In principle, the equilibrium value of dn/dc could be obtained after dialysis of the solution against a solvent of a constant composition. Unfortunately, such dialysis is not feasible with surfactants since the micelles can dissociate and can thus pass the semipermeable membrane. The problem will be discussed below in more detail.

Theoretical

The technique of static light scattering (SLS) is described in many textbooks of polymer science, and rather comprehensive literature is collected in Huglin's book [21]. Similarly, a detailed outline of dynamic light scattering (DLS)

Colloid & Polymer Science, Vol. 273, No. 9 (1995)

is found in the book of Berne and Pecora [18]. For this reason only the main concepts are outlined in the present paper.

Static LS

Measurements in dilute solutions are commonly evaluated on the basis of the Debye equation

$$K_c/R_\theta = [1/(M_w P_z(q))] + 2A_2 c \,, \quad (1)$$

where c is the surfactant concentration (w/vol), M_w the mass-average molar mass of the colloidal particle, A_2 the second virial coefficient and $P_z(q)$ is the particle scattering factor with $q = (4\pi n_0/\lambda_0)\sin(\theta/2)$, θ being the scattering angle. K is an optical contrast factor which is given by

$$K = 4\pi^2/(N_A \lambda^4) n_0^2 (dn/dc)^2 \,, \quad (2)$$

where N_A denotes Avogadro's number, λ_0 the wavelength of light in vacuum, n_0 the solvent refractive index, and dn/dc the refractive index increment.

For particles with dimensions smaller than the wavelength of light the particle scattering factor can be expanded in terms of the scattering vector q^2

$$1/P_z(q) = 1 + (1/3)q^2 R_g^2 + \cdots \,, \quad (3)$$

where R_g is the radius of gyration of the dissolved particle. This radius is geometrically defined and represents the average distance of scattering units inside the particle from the center of mass. Equations (1) and (2) are the basis for the static Zimm plot in which K_c/R_θ is plotted against $q^2 + kc$ with k as arbitrary constant. An example of such a plot is shown in Fig. 1. From this plot three molecular parameters can be obtained, i.e., $1/M_w$ from the intercept with the ordinate of the curves at $c = 0$ and $q = 0$, the radius $R_g (= [\langle S^2 \rangle_z]^{1/2})$ from the slope of the angular, i.e., q^2-dependence at the concentration $c = 0$, and the second virial coefficient A_2 from the concentration dependence of the scattered intensity at zero angle. The last parameter gives valuable information on the interaction between particles and can be expressed in terms of an equivalent hard-sphere radius of the dissolved colloidal particle [22, 23]

$$R_{eq} = \{(A_2 M_w^2)[(3/(N_A 16\pi)]\}^{1/3} \quad (4)$$

This equivalent radius is a thermodynamically defined radius which differs from the geometrically defined radius of gyration R_g. The difference between these two radii is characteristic of the particle architecture (note, however, comments made in the discussion).

Fig. 1 Zimm plot from the light-scattering measurements of *n*-hexadecylammonium hydrogensulphate in concentrated sulphuric acid (96%)

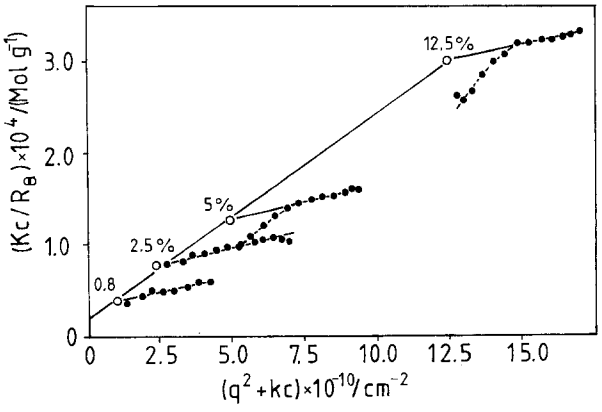

Dynamic LS

In contrast to static LS the scattering intensity in dynamics LS is measured in very short time intervals from about 10^{-6} s up to about 100 s. This intensity fluctuates strongly with the elapsed time and cannot be directly evaluated. Dynamic quantities can be obtained, however, from the scattering intensity time correlation function $G_2(t)$ (TCF) which is given as follows

$$G_2(t) = \langle i(0) i(t) \rangle = A + B[g_1(t)]^2 \,, \quad (5)$$

in which $g_1(t)$ is the electric field TCF given by

$$g_1(t) = |\langle E^*(0) E(t) \rangle| / |\langle E^*(0) E(0) \rangle| \,, \quad (6)$$

In these equations $i(t)$ denotes the scattering intensity at a time t and $i(0)$ that at zero time, i.e., at the beginning of the measurements. Similarly, $E(t)$ is the corresponding electric field of the scattered light at the time t and $E^*(t)$ the corresponding conjugate complex quantity.

Hence, in a TCF a fluctuating quantity at time t is compared with that at $t = 0$. The TCF of the intensity decays exponentially in time towards a baseline A, while that of $g_1(t)$ decays to zero. In the simple case of hard spheres the TCF decays like a single exponential curve

$$g_1(t) = B \exp(-q^2 D t) \quad (7)$$

Accordingly, the slope in a plot of $\ln(g_1(t))$ against t is

$$\Gamma = q^2 D_c \,, \quad (8)$$

which allows the determination of the translational diffusion coefficient D_c at concentration c. Mostly, however, the plot of the logarithmic TCF against t shows deviations from a straight line, but the initial slope is still given by Eq. (8). In order to find this initial slope Γ_1, a so-called cumulant fit [24] is applied, i.e., the curve is fitted by a cubic

equation

$$\ln[g_1(t)] = \ln(\Gamma_0) - \Gamma_1 t + (\Gamma_2/2)t^2 - (\Gamma_3/6)t^3 , \quad (9)$$

where Γ_i is the i-th cumulant with $i = 1, 2, 3$. At infinite dilution the ratio Γ/q^2 becomes the translational diffusion coefficient D_0 for which we can write:

$$D_0 = kT/(6\pi\eta_0 R_h) . \quad (10)$$

This Stokes–Einstein relationship defines a hydrodynamically effective radius $R_h = [\langle 1/r_h \rangle_z]^{-1}$; r_h is the hydrodynamic radius of a monodisperse material of a well-defined molar mass and the subscript z denotes the z-average. In general, the diffusion coefficient depends on concentration and often can be described in a wide range of concentration by a linear equation, i.e., $D_c = D_0(1 + k_D c)$.

The hydrodynamic radius differs from the radius of gyration R_g and the ratio $\rho = R_g/R_h$ is a characteristic parameter of the particle architecture. For hard spheres one has $\rho = 0.778$. The values for other architectures [19] are given in Table 1 and will be discussed in the context of the experimental section 5.

The deviations of the TCF from a straight line can be caused by polydispersity, and for very large particles, also by internal modes of motion. Sometimes this distribution is very broad, and in such cases it is more sensible to plot the linear function $g_1(t)$ against the logarithm of time. A typical example, obtained from a fairly concentrated solution, is given in Fig. 2. Clearly two processes are seen.

It seems that a third, very slow process is present which could not be fully resolved. The TCF has not decayed to a zero base line, but leveled off at a constant value of 0.03.

Fig. 2 Field time correlation function plotted against the logarithm of delay time from a 20% solution of *n*-hexadecylammonium hydrogensulphate in concentrated sulphuric acid measured at scattering angle of 90 degrees. The TCF shows clearly the presence of two relaxation processes

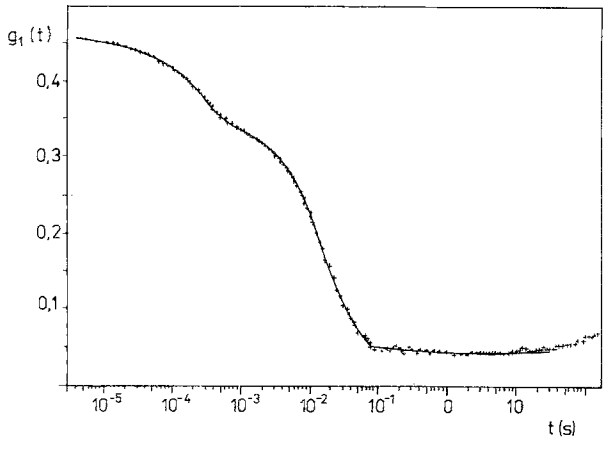

This small deviation from the zero base line may be simply the result of experimental error. In any case the effect is small and will not cause a strong distortion by heterodyne scattering. The effect has been neglected in the following and the measured base line was taken as the true one.

Results

Static light scattering

Light-scattering measurements were performed with concentrations of 0.8, 2.5, 5.0, 7.5, 10, 12.5 and 20% (w/vol) at a temperature of 20 °C. In the beginning these solutions were filtered through 0.2 μm Teflon filters. In the course of our experiments, we noticed some uncommon behavior that seemed to indicate a pronounced clustering of particles. Therefore, the higher concentrations were filtered through 0.5 μm filters which now gave consistent results. All scattering measurements were carried out at various angles from 30 to 150 degrees in steps of 10 degrees. These results were extrapolated towards zero scattering angle.

Figure 1 shows the result from four concentrations which were filtered through the small pore size filters (0.2 μm). Parallel lines were obtained in the wide-angle region ($\theta > 80$ degrees) for the two high concentrations with strong deviations towards lower values in the low scattering angle region. This low angle excess scattering gives strong indications for the presence of large aggregates which were not fully separated by filtration. Therefore, the LS measurements were repeated with solutions that were filtered through the large pore size (0.5 μm). A much stronger scattering was then observed.

No excess scattering was observed with the two lowest concentrations. Unfortunately, no reliable results could be obtained at scattering angles $\theta > 100$ and 120 degrees, respectively, because of the very small difference in the scattering intensities of the solvent and the solution in that region.

Both sets of curves, those filtered through 0.2 μm and the others filtered through 0.5 μm pore size, could be linearly extrapolated to zero scattering angle. An exception was recorded with the highest concentration (20%) where a slight upturn at large scattering angles was observed (see Fig. 5). The data of this forward-scattering are shown in Fig. 3. It is of interest that the data points from the 0.2 μm filtered solutions fall on a straight line that can be extrapolated to zero concentration. The intercept gives an apparent molar mass $M_w^* = 45\,500 \pm 4.5\%$ and the slope of the straight line gives an apparent second virial coefficient $A_2^* = 1.11 \times 10^{-3}$ mol cm^3/g^2 with an error of about $\pm$ 10%. These two quantities may be distorted by

Colloid & Polymer Science, Vol. 273, No. 9 (1995)

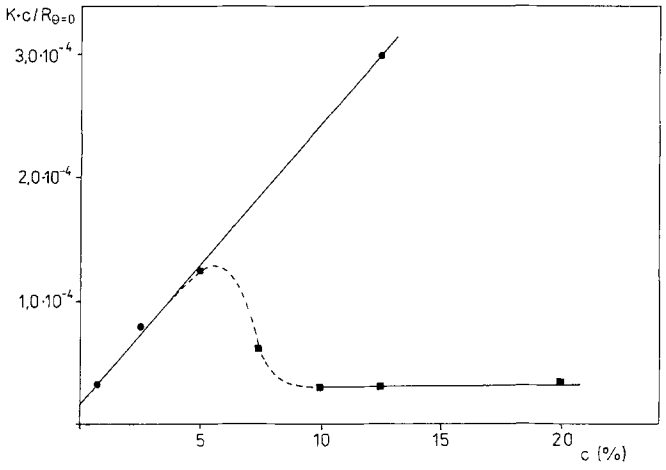

Fig. 3 Forward-scattering (obtained by extrapolation to zero scattering angle) of *n*-hexadecylammonium hydrogensulphate in dependence on the concentration of the surfactant. Filled circles: filtered through 0.2 μm pore size, filled squares: filtered through 0.5 μm Teflon filters

the effect of preferential adsorption of water, and therefore the quantities are indexed by an asterisk.

The corresponding radius of gyration can be obtained from the slope at zero concentration in the Zimm plot of Fig. 1 and was found to be 76.2 nm. This value was cross-checked by determining the apparent radii of gyration at different concentrations and extrapolation of these data to zero concentration with estimated error of $\pm 5\%$. The curves of the solutions filtered through the large pore sizes exhibited a strong angular dependence with a linear angular dependence that changed to a slight upturn at the largest concentration (Fig. 5). This upturn indicates a change to a fairly compact structure.

The evaluation of Zimm plots offers no serious difficulties with covalently linked structures of synthetic polymers. A question arises, however, about whether the same technique can applied to micellar structures which may grow in size as the concentration is increased [15]. Here, we have to recall that the predominant and sudden change in structure occurs around the CMC. At higher concentrations the structures grow only slowly even for rod-like micelles. The type of length distribution is not changed thereby, but remains a most probable distribution with a heterogeneity factor of $L_w/L_n = 2$ [15, 16].

Since the CMC is much smaller than the lowest applied concentration, we are not able to observe the dissociation into the unimers below the CMC. The Kc/R_θ data extrapolated to $c = 0$ corresponds very closely to those at the lowest concentration, but without the distortion due to thermodynamic interactions among the dissolved objects. Similar results were found earlier with micelles in aqueous media [11, 12].

Dynamic LS

All dynamic LS measurements were performed with solutions filtered through 0.5 μm pore size filters. The translational diffusion coefficients as a function of the concentration D_c, shown in Fig. 4 (open circles), were determined from the initial slope in a three cumulant fit as described by Eq. (9). In addition, data are shown which correspond to the fast motion that was obtained by the analysis of the time correlation function. A typical example is shown in Fig. 2.

In order to separate the fast from the slow motion, we performed a fitting analysis with Kohlrausch–Williams–Watts [34] functions, which have the general form,

$$g_{1i}(t) = a_1 \exp[-(t/\tau_i)^{\beta i}]; \quad i = 1,2\,. \tag{11}$$

The mean relaxation time of this function is given by

$$\langle\tau\rangle_i = [1/\Gamma(\beta_i)]\,(\tau_i/\beta_i); \quad i = 1,2\,, \tag{12}$$

where $\Gamma(\beta_i)$ is the common gamma function. The corresponding apparent translational diffusion coefficient is given by

$$D_{app,i}(q) = 1/(q^2\langle\tau\rangle_i)\,. \tag{13}$$

The coefficients a_i, which correspond to the mass fractions of associated and non-associated micelles, and the $D_{app,i}(q)$ depend on the scattering angle and have to be extrapolated to $\theta = 0$. The results are given in Table 2. The filled circles in Fig. 4 represent $D_c(q = 0)$ for the fast motion,

Fig. 4 The translational diffusion coefficient D_c as a function of concentration of the surfactant in concentrated sulphuric acid (96%). The open circles correspond to the cumulant fits; the filled circles represent the fast motion in the system which was found from the analysis of the TCF with a Kohlrausch–Williams–Watts function. The open squares refer to the slow motions

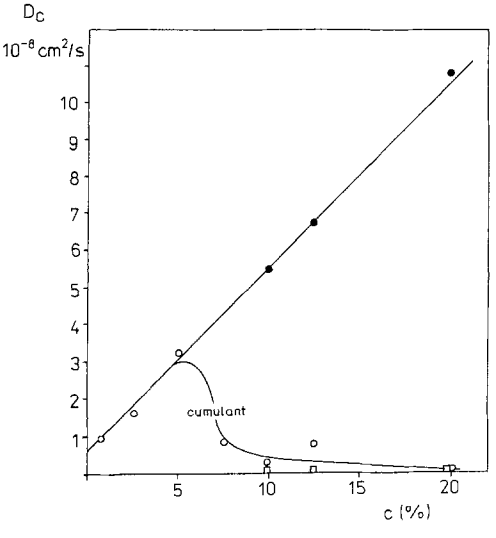

while the data of the slow motion are shown as open squares.

Discussion

The discussion may be separated in two parts corresponding to the small and the large particles.

Micellar structure

The data for the molar mass M_w^*, the second virial coefficient A_2^* and the two radii (R_g and R_h) are listed in Table 3 where the asterisks indicate quantities which may be distorted by a preferential adsorption of water. We start the discussion with the three quantities which can be measured and interpreted without having knowledge of the true molar mass. These are the two radii R_g and R_h and the resulting ratio $\rho = R_g/R_h$. Table 1 gives a list for various architectures. From this, we immediately come to the conclusion that rather rigid and elongated structures must be present. However, the ρ-parameters also depend on polydispersity, and the effect is particularly strong for rodlike structures. In Appendix 1 a mathematical derivation is given for the dependence of the ρ-parameter on the axial ratio of cylinders and on their polydispersity, where Schulz–Zimm [35, 36] type distributions have been used. Mostly, associating rods follow the Schulz–Flory [36, 37] length distribution ($L_w/L_n = 2$, with w and n indicating the weight and number averages, respectively). For this distribution, we find (see Appendix 1)

$$\rho = 0.92278 + \ln(p_w/2) \tag{14}$$

and

$$L_w = 2[\langle S_2 \rangle_z]^{1/2} = 2R_g\,. \tag{15}$$

With these data, we obtain $p_w = 60.4$, $L_w = 152$ nm and a cross-sectional diameter $d = 2.53$ nm with estimated errors of about 5–10%.

Knowing the length L_w and diameter d of the cylinder, we can now estimate to what extent the measured apparent molar mass M_w^* might be distorted by a possible preferential adsorption of water. To that, we apply a relationship for the second virial coefficient derived by Yamakawa [22], which may be written as

$$(A_2 M_w^2)_{cal} = (\pi/4)\, N_A\, d\, L_w^2\,. \tag{16}$$

Inserting the values from Table 3 for L_w and d, we find $(A_2 M_w^2)_{cal} = 27.8 \times 10^6$ cm^3, while experimentally we found $(A_2^* M_w^{*2}) = 2.3 \times 10^5$ cm^3. Furthermore, it can be shown [38] that

$$A_2^* M_w^* = A_2 M_w\,, \tag{17}$$

such that the correct molar mass M_w would be larger by a factor 12.1 than M_w^*. This difference between measured and correct M_w would correspond to a change in dn/dc due to preferential adsorption from 0.039 to 0.011. Because of the large difference in the refractive indices of water and concentrated sulphuric acid such a variation would be caused by a fairly weak preferential adsorption to the surfactant and appears well conceivable. On the other hand, the small difference in dn/dc values could be the result of experimental error. We are aware of the speculative character of the conclusions. However, further structure parameters can now be estimated, and these appear realistic and sensible. The results may justify the applied speculative argumentation.

Table 1 Values of the two ratios of radii $\rho = R_g/R_h$ for various molecular architectures. $p = L/d$ is the axial ratio of a cylinder and the w indicates the weight average

	ρ	Ref.
Random coils	1.27–2.05	[19, 26, 30]
Star molecules	1.50–1.02	[19, 28, 29)]
Spheres	0.778	–
Microgels	0.3–0.55	[31]
Rods	> 2.2[a)]	[21, 32, 33]

[a)] Monodisperse cylinders $\rho = 0.577 \ln p$ (Ref. 3B)
Polydisperse rods ($L_w/L_n = 2$) $\rho = 0.92278 + \ln(p_w/2)$ (appendix 1)

Table 2 Diffusion coefficients of the slow and fast motions and the corresponding prefactors a_1 and a_2 after extrapolation to zero scattering angle

c (% w/vol)	D_1(slow) (cm^2/s)	a_1	D_2(fast) (cm^2/s)	a_2
20.0	5.7×10^{-10}	0.98	7.4×10^{-8}	0.02
12.5*	8.3×10^{-10}	0.80	6.9×10^{-8}	0.20
10.0	8.1×10^{-10}	0.95	5.6×10^{-8}	0.05

*) filtered through 0.2 μm pore size

Table 3 Molecular parameters obtained from static and dynamic light scattering and estimated rod length L and axial ratio $p = L/d$ assuming rigid rod behavior

Molar particle mass	$M_w^* = 45\,500 \pm 4.5\%$
Aggregate second virial coefficient	$A_2^* = 1.11 \times 10^{-3}$ mol cm^3/g^2
Diffusion coefficient	$D_0 = 0.52 \times 10^{-8}$ cm^2/s
Radius of gyration	$R_g = 76.2$ nm
Rod length	$L_w = 152.6$ nm
Hydrodynamic radius	$R_h = 17.7$ nm
Ratio $\rho = R_g/R_h$	$\rho = 4.33$
Axial ratio	$p_w = 60.4$
Cylinder diameter	$d = 2.53$ nm

Colloid & Polymer Science, Vol. 273, No. 9 (1995)

It is interesting to compare R_{eq}, derived from Eq. (4), with the hydrodynamic radius that is obtained from the Stokes–Einstein relationship, Eq. (10). The value of $R_{eq} = 14$ nm is 26% lower than $R_h = 17.7$ nm. For flexible linear chains $R_{eq} \cong R_h$ was found [27]. In view of the fairly high uncertainty in the determination of A_2 in the present case, the observed 26% deviations can be considered as a reasonable agreement and correspond to the expected behavior of rigid rods.

Assuming $M_w = 5.5 \times 10^5$ g/mol being the correct molar mass of the micelle, one obtains with the surfactant molar mass of $M_0 = 339$ g/mol an aggregation number of $n = 1620$ and a linear mass density of $M_L = M_w/L_w = 3.6 \times 10^3$ g/(mol nm). We may now ask how large the average distance l is between slices which contain m surfactant unimers, and furthermore, whether there exsists a physically acceptable number m for which the average distance l between slices is the same as for two head groups on the circumference of a circular disc. The answer is found from the relationships

$$m = (\pi\, dn/L_w)^{1/2} \quad l = \pi d/m$$

which are obtained by simple algebra. The result is

$$m = 9.2 \quad \text{and} \quad l = 0.87 \text{ nm} .$$

We thus come to the conclusion that approximately nine surfactant molecules are arranged on a circular slice and that 176 of these slices form the cylinder. The space required on average by one head group is spanned by a radius of 0.43 nm. The cylinder is probably not completely rigid but can undergo some bending motions. Because of the fairly short length compared to the wavelength of the light used, this remaining flexibility could not be determined. The circular diameter d appears about half as large as expected for two tail-to-tail aligned surfactant unimers. However, the mean distance $l = 0.86$ nm between head groups as found by analysis of light scattering data is close to the value that was found earlier from surface tension and Gibbs adsorption measurements on a surface of the same surfactant in sulphuric acid.

Structure at high concentrations

The high axial ratio, found from experiments with assumption of a most probable length distribution, should have some interesting consequences for the solution structure in moderately concentrated solution. Considering a rather simple model, Flory [39] derived a criterion at what volume fraction Φ a mesophase transition to an optically anisotropic solution could be expected. The relationship is given by

$$\Phi^* = (8/p)(1 - 2/p) . \tag{18}$$

With the axial ratio of $p_w = 60.4$, we find $\Phi^* = 0.128$, which would correspond to a concentration of approximately $c^* = 12$–13% (w/v), assuming a surfactant density of about 1 g/ml. Therefore, some uncommon effects may be expected in the vicinity of this concentration.

There is a striking similarity between the two Figs. 3 and 4. In both cases a turn-over to smaller values occurs at concentrations of about 5%. Evidently, a transition to another aggregation structure occurs. The transition takes place in the fairly narrow region between 5 and 10%. Beyond these concentrations no dramatic increase of the particle weight is recognized. The angular dependence of the scattered intensity at 20% shows a significant upturn curvature which is characteristic for globular structure (Fig. 5) Therefore, we can conclude that a lateral aggregation of the micellar rods takes place at concentrations higher than 5%.

These findings confirm to some extent the expectations drawn from Flory's theory that a mesophase is formed,

Table 4 Molecular parameters resulting from the correction of M_w^* for the correct molar mass of the cylinders

Molar mass	$M_w = 548\,000$
Second virial coefficient	$A_2 = 0.91 \times 10^{-4}$ mol cm^3/g^2
Molar mass of surfactant	$M_0 = 339$ g/mol
Linear mass density	$M_L = 3600$ g/(mol nm)
Aggregation number	$n = 1620$
Number of surfactants per slice	$m = 9.2$
Number of stacked slices	$n/m = 176$
Distance between head groups	$l = 0.87$ nm
Predicted critical volume fraction for mesophase transition	$\Phi^* = 0.128$

Fig. 5 Angular dependence of the scattered intensity from a 20% solution of the surfactant in concentrated sulphuric acid (96%)

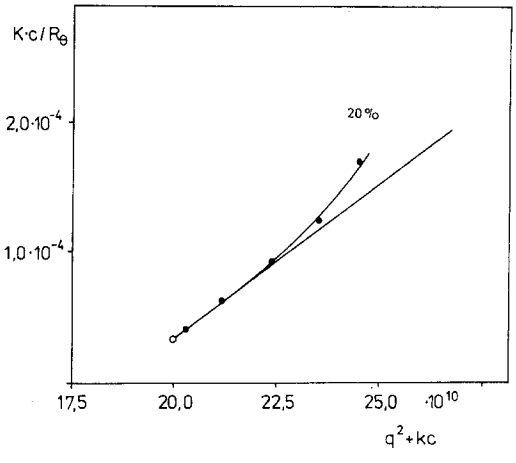

and that this mesophase is anticipated by a lateral aggregation of micellar rods. Due to the low scattering intensity, we have not yet been able to measure the depolarized scattering intensity R_{vh} which would give a proof for the suggested onset of a mesophase transition.

The similar behavior of the concentration dependence of D is easily explained by irreversible thermodynamics giving the following equation (20)

$$D_c = (kT/f_c)[M(c)/M_{app}(c)] , \tag{19}$$

with

$$1/M_{app}(c) = (Kc/R_\theta)_c . \tag{20}$$

The true molar mass of the particle at concentration c is denoted by $M(c)$ and the concentration dependence of the friction coefficient by f_c. The similarity of Figs. 3 and 4 demonstrates that the molar mass $M(c)$ and the friction coefficient f_c increase approximately to the same magnitude such that the ratio $M(c)/f_c$ remains almost constant.

The apparent diffusion coefficient $D_{app} = \Gamma_1/q^2$ is often angular dependent which is an indication of some internal flexibility. Such angular dependence was also observed at concentrations from 5 to 12%. However, a very low diffusion coefficient and no angular dependence at all was found at 20%. This indicates a very inflexible, almost spherical structure, since extended rods display an angular dependence even if they are completely rigid [18, 19]. This conclusion is consistent with the findings from the angular dependence of static scattering.

Conclusion

1. This light scattering study demonstrates that common cationic surfactants form micellar structures also in concentrated sulphuric acid.
2. The *n*-hexadecylammonium hydrogensulphate forms rodlike micelles with an axial ratio of 60 in 96% H_2SO_4.
3. The micelle is built up by 176 slices each containing about six surfactant molecules.
4. At concentrations higher than 5% surfactant the rod micelles cluster together to form more globular structures.
5. The time correlation functions recorded by dynamic light scattering at high concentrations exhibited a two-step decay. This behavior is indicative of the presence of a bimodal distribution of particle sizes. The fast motion agrees with the motion of the individual micelles observed at low concentrations. The other motion, which is slower by 3 orders of magnitude than the fast one, corresponds to the translational motion of larger clusters.
6. The results at concentrations larger than 5–10% are in fair agreement with Flory's prediction for the onset of a mesophase transition when cylinders of the indicated axial ratio are present.

Acknowledgement We thank Dipl. Chem. Frank Jenne for his help in many details to perform the uncommon LS experiments and to overcome the difficulties involved with the sulphuric acid. We also thank Prof. Manfred Schmidt, University of Bayreuth for drawing our attention to the significant influence of polydispersity on the ρ-parameter. This joint work would not have been possible without the financial support of the Fonds of Chemical Industry, Frankfurt, Germany which A.M. gratefully acknowledges. Part of the work was also kindly supported by the Deutsche Forschungsgemeinschaft.

Appendix 1: The rho-parameter of polydisperse cylinders as a function of the axial ratio

The here derived equations are similar to those given by Schmidt [40] in his contribution on wormlike chains; he used Broersma's equation for cylinders instead of Kirkwoods' relationship.

The translational diffusion coefficient of monodisperse cylinders, built up of N beads of diameter b, was calculated by Riseman and Kirkwood [33], and is given as

$$D_{rod} = (kT/N\zeta)\{1 + (\zeta/3\pi\eta_0 b)[\ln(N) - 1] . \tag{A1}$$

Setting the frictional coefficient of one bead as $\zeta = 3\pi\eta_0 b$ and defining the hydrodynamic radius via the Stokes–Einstein relationship, we obtain

$$R_h^{-1} = \langle 1/r_h \rangle = (2/L)\ln(L/b) = (2/L)\ln p . \tag{A2}$$

Since the radius of gyration of long cylinders is

$$R_g = L/(12)^{1/2} = 0.57735(L/2) , \tag{A3}$$

we find for the ρ-parameter of monodisperse cylinders

$$\rho = R_g/R_h = 0.57735 \ln p . \tag{A4}$$

Now, the length distribution of such cylinders may be of the Schulz–Zimm [35, 36] type [36, 37]

$$w(L) = (y^{z+1}/z!)L^z \exp(-yL) , \tag{A5}$$

with

$$y = (z + 1)/L_w , \tag{A6a}$$

and

$$z = [(L_w/L_n) - 1]^{-1} . \tag{A6b}$$

Thus, we have

$$\langle L^2 \rangle_z = \left[\int_0^\infty L^3 w(L) dL\right]/L_w , \tag{A7}$$

and

$$1/R_h = \langle 1/r_h \rangle_z = \left[\int_0^\infty 2\ln(L/b) w(L) dL\right]/L_w . \tag{A8}$$

Colloid & Polymer Science, Vol. 273, No. 9 (1995)

Table A1 Relationships for the polydispersity and axial ratio dependence of the ρ parameter of rigid cylinders. $z = (L_w/L_n - 1)^{-1}$ polydispersity factor in the length distribution of Eq. (A5), $p_w = L_w/d$ axial ratio with L_w as the long axis and the cylinder diameter d as the short axis

z	L_w/L_n	$\rho = [\langle R_g^2\rangle_z]^{1/2}\langle 1/R_h\rangle_z$	ρ_{10} [a]	ρ_{100} [a]
1	2.0	$0.92278 + \ln(p_w/2)$	2.532	4.84
2	1.5	$0.8607[1.2561 + \ln(p_w/3)]$	2.117	4.10
5	1.2	$0.7200[1.8728 + \ln(p_w/6)]$	1.7162	3.37
10	1.1	$0.6555[2.4426 + \ln(p_w/11)]$	1.5386	3.048
∞	1.0	$0.5777 \ln(p)$	1.329	2.658

[a] the subscripts denote the axial ratio

Inserting Eq. (A5) into Eqs. (A7) and (A8), and solving the resulting integrals analytically [40, 41] gives

$$R_g = [\langle L^2\rangle_z/12]^{1/2} = [(z+3)(z+2)/(12(z+1)^2]^{1/2} L_w , \quad \text{(A9)}$$

and

$$1/R_h = \langle 1/r_h\rangle_z = (2/L_w)[\Psi(z+1) + \ln\{L_w/[(z+1)b]\} , \quad \text{(A10)}$$

and finally

$$\rho = [(z+3)(z+2)/3(z+1)^2]^{1/2}\{0.4287 + 1/2 + 1/3 + \cdots + \ln[p_w/(z+1)]\} , \quad \text{(A11)}$$

where we have used a property of the Ψ-function [41]

$$\Psi(z+1) = 1 - E + 1/2 + \cdots + 1/(z+1)$$

with the Euler constant $E = 0.57722$. In particular for $z = 1$ (Schulz—Flory distribution) [35, 37], we have

$$\rho = 0.92287 + \ln(p_w/2) , \quad \text{(A12)}$$

which has been used in the text. Table A1 gives a list of relationships for some selected polydispersities.

Appendix 2: Correction for the second virial coefficient

Since ref. [38] is not easily available, for convenience Eq. (18) is derived here again. Let us assume that incorrect values for dn/dc have been used for the calculation of the absolute scattering intensity. This would result in an equation of

$$K^*c/R_{\theta=0} = 1/M_w^* + 2A_2^*c + \cdots . \quad \text{(A13)}$$

while the correct relationship is

$$Kc/R_{\theta=0} = 1/M_w + 2A_2c . \quad \text{(A14)}$$

Since K^* differs from K only by a constant, we can multiply Eq. (A13) by a factor M_w^*/M_w which results in

$$[1/M_w^* + 2A_2^*c](M_w^*/M_w) = 1/M_w + 2A_2^*(M_w^*/M_w)c . \quad \text{(A15)}$$

Comparing Eq. (A14) with Eq. (A15), we find

$$A_2^*M_w^* = A_2M_w , \quad \text{(A16)}$$

which has been used in the text.

References

1. Menger FM, Jerkunica JM (1979) J Am Chem Soc 101:1896
2. Yan FJ, Palmer MB (1969) Colloidal Interface Sci 30:177
3. Gillespie BE, Smith MJ, Wyatt PAH (1969) J Chem Soc p 304
4. Steigmann J, Shane N (1965) J Phys Chem 69:968
5. Müller A (1991) Colloids Surfaces 57: 227
6. Müller A, Miethchen R (1988) J Prakt Chem 330:993
7. Müller A (1991) Colloids Surfaces 57:219
8. Müller A (1991) Colloids Surfaces 57:239
9. Müller A, Giersberg S (1991) Colloids Surfaces 60:389
10. Müller A, Giersberg S (1992) Colloids Surfaces 69:5
11. Richtering WH, Burchard W, Jahns E, Finkelmann H (1988) J Phys Chem 89: 6032
12. Denkinger P, Burchard W, Kunz M (1989) J Phys Chem 93:1428
13. Richtering WH, Löffler R, Burchard W (1992) Macromolecules 25:3642
14. Richtering WH, Schätzle J, Adams J, Burchard W (1989) Colloid Polym Sci 267:568
15. Candau SJ (1987) in: Surfactant Solutions-New Method of Investigation, Ed Zana R, Dekker M Inc, New York, pp 147–207
16. Magid L (1993) in: Dynamic Light Scattering, Ed Brown W, Oxford Science Publ, Oxford, pp 554–589
17. Bantle S, Schmidt M, Burchard W (1982) Macromolecules 15:1604
18. Berne BJ, Pecora R (1976) Dynamic Light Scattering, Wiley New York
19. Burchard W, Schmidt M, Stockmayer WH (1985) Macromolecules 13:588
20. D'Ans-Lax (1967) Taschenbuch für Chemiker und Physiker, Springer, Berlin-Heidelberg
21. Huglin MB (1972) Light Scattering from Polymer Solutions, Academic Press, London-New York
22. Yamakawa H (1971) Modern Theory of Polymer Solutions, Harper & Row, New York
23. Burchard W (1992) in: Polysaccharide, Ed Franz G, Springer Verlag, Heidelberg
24. Koppel DE (1972) J Chem Phys 57:4814
25. Goldstein M (1953) J Chem Phys 21:1255
26. Rey A, Freire JJ, Garcia de la Torre J (1987) Macromolecules 20:242

27. Huber K, Burchard W, Akcasu ZA (1985) Macromolecules 18:274
28. Rey A, Freire JJ, Garcia de la Torre J (1990) Macromolecules 23:3948
29. Lang P, Burchard W, Wolfe MS, Spinelli HJ, Page L (1991) Macromolecules 24:1306
30. Akcasu ZA, Benmouna M (1978) Macromolecules 11:1178
31. Schmidt M, Nerger D, Burchard W (1979) Polymer 20:582
32. Burchard W (1986) in: Cyclic Polymers, Ed Semlyen JA) Elsevier, London-New York
33. Riseman J, Kirkwood JG (1950) J Chem Phys 18:512
34. Williams G, Watts DC (1970) Trans Faraday Soc 60:80
35. Schulz GV (1939) Z Physikal Chem B 43:25
36. Zimm BH (1948) J Chem Phys 16:1093
37. Flory PJ (1936) J Amer Chem Soc 58:1877
38. Huisman HF (1964) Koningl Ned Akad Wetenschap Proc Ser B 64:367
39. Flory PJ (1956) Proc Roy Soc London A234:73
40. Schmidt M (1984) Macromolecules 17:553
41. Groebner W, Hofreiter N (1958) Integraltafel, 2. Teil: Bestimmte Integrale, Springer-Verlag, Wien-Insbruck, Eq. 324–383, p 81